

Selective Interaction of $\beta 3$ Integrin with Guanine Nucleotide-Binding Proteins $G\alpha 12$ and $G\alpha 13$

Jane Warstler
Cell and Molecular Biology
The University of North Carolina Asheville
One University Heights
Asheville, NC 28804 USA

Faculty Advisor: Dr. Thomas E. Meigs

Abstract

Cell attachment, migration, and proliferation are essential processes for both normal tissue growth and malignant development of cancers. Guanine nucleotide-binding (G) proteins and cell surface proteins of the integrin family play key roles in the regulation of these processes. The G proteins $G\alpha 12$ and $G\alpha 13$ have 66% amino acid homology, yet differ in their downstream signaling function. While these proteins have been extensively studied in their own roles, the mechanisms by which they interact have only been partially examined. Other investigators have shown C-terminal binding of $\beta 3$ integrin to $G\alpha 13$, but not $G\alpha 12$. In the Meigs lab, G protein affinity for $\beta 3$ integrin was examined utilizing epitope-tagged forms of $G\alpha 12$ and $G\alpha 13$. It was found that $G\alpha 12$ showed greater binding affinity for $\beta 3$ integrin than did $G\alpha 13$, in both myc- and GFP-tagged forms. Furthermore, constitutively active and inactive forms of $G\alpha 12$ and $G\alpha 13$, as well as wild-type $G\alpha 12/13$, were utilized to determine if this differential was affected by the activation state. For $G\alpha 12$, $\beta 3$ integrin exhibited stronger binding for the GTP-bound form than the wild-type or GDP-bound forms. These findings suggest that $G\alpha 12$ must be in the GTP-bound form to adequately bind $\beta 3$ integrin in cells. In regards to $G\alpha 13$, $\beta 3$ showed strongly impaired binding in all activation states. Lastly, NAAIRS sextet mutations were tested to attain greater knowledge of specific structural features of $G\alpha 12$ required for interaction with $\beta 3$ integrin¹. Unexpectedly, two sextet amino acid substitution mutants of $G\alpha 12$ exhibited impaired binding to $\beta 3$ integrin. This provides new structural details and serves as a basis for further research in examining these regions to specifically identify the properties that disallow binding action. As both $G\alpha 12$ and $G\alpha 13$ have been implicated in cancer pathways, understanding these interactions is critical for complete mechanistic understanding of the metastatic potential of epithelial cancer cells.

1. Introduction

Heterotrimeric guanine nucleotide-binding (G) proteins play essential roles in cancer progression, metastatic invasion, and embryonic development. Better understanding of the cellular signaling processes that allow these to occur is integral for the future of potential antineoplastic drugs. These proteins consist of α , β , and γ subunits, which rely on GDP-GTP exchange for activation². Upon activation, the α subunit dissociates with the β/γ subunits and serves as the major signaling molecule for its downstream effectors³. $G\alpha 12$ and $G\alpha 13$ are members of the G12/13 class of these proteins. While these proteins have similar sequence homology, they invoke distinct downstream signaling processes. $G\alpha 13$ has been shown to interact with and regulate the function of $\beta 3$ integrin, but there is little data on the $G\alpha 12/\beta 3$ integrin interaction published⁴.

Integrins are heterodimeric integral transmembrane protein receptors consisting of α and β subunits, with a large extracellular domain and a small cytoplasmic tail. They are heavily involved in cell surface-mediated signaling, specifically between the actin skeleton and extracellular matrix during cell migration. Likewise, they play a critical role in thrombosis and hemostasis, which involves outside-in signaling related to platelet spreading⁵. Integrins

participate in two different types of signaling: outside-in and inside-out. This inside-out signaling activates ligand binding, and cellular stimulation triggers clustering or altered conformation of the integrin subunits to increase their affinity for ligands⁴. Outside-in signaling then mediates the responses induced by the ligand binding, and “signals are transduced to the cytoplasm, which induces a cascade of intracellular signaling events, including protein phosphorylation and cytoskeletal reorganization”⁶. Downstream effects of this signaling also include spreading, retraction, migration and proliferation.

The impetus for this research began with findings that outside-in and inside-out signaling both require G protein interaction, and that crosstalk occurs between G-protein coupled receptors (GPCR) and $\beta 3$ integrin pathways². Furthermore, Gong *et al.* elucidated that $\alpha 13$ -integrin interaction was supported in the GTP-bound, constitutively active form of $\alpha 13$, through binding at the cytoplasmic domain of $\beta 3$ integrin⁷. Given that cadherins have been shown to interact robustly with both G protein families, the commonalities of cadherins and integrins in the $\alpha 12/13$ domains used for binding were examined. A comparative binding study of $\alpha 12$ versus $\alpha 13$ was performed, and the structural determinants that evolved to allow binding and regulation of $\beta 3$ integrin were examined. Furthermore, it was sought to determine whether the activation state of the G proteins had any effect on binding affinity. Cassette mutational analysis was employed to identify the regions of $\alpha 12$ necessary for $\beta 3$ integrin binding, as well as epitope-tagged variants of $\alpha 12$ and $\alpha 13$.

2. Materials and Methods

2.1 Creation of GST $\beta 3$ Integrin Fusion

Based on the recent finding of Gong *et al.* that the cytoplasmic domain of $\beta 3$ integrin interacts with $\alpha 13$, this domain was examined for interaction with $\alpha 12$ in comparison to $\alpha 13$ ⁴. GST-fusions were created by polymerase chain reaction (PCR)-amplifying the amino acids comprising this cytoplasmic tail of $\beta 3$ -integrin from human and mouse brain cDNA libraries. Published sequences for human (GenBank: AGC54784.1) and mouse (AAB94086.1) $\beta 3$ integrin were examined and oligonucleotides were selected to hybridize to amino acid sequences 742-788 and 741-787, respectively. Flanking this amplicon, BamHI (upstream, 5'-GGATCC-3') and Sall (downstream, 5'-CAGCTG-3') restriction endonuclease sites were engineered to allow ligation into pGEX-5X-1 plasmid vector (GE Healthcare). Two arbitrary nucleotides were added in the forward primer between the BamHI and $\beta 3$ integrin start codon site in order to preserve the correct reading frame for the protein. Likewise, a stop codon was introduced in the reverse primer. The PCR oligonucleotides used (Eurofins Genomics) are as follows:

Human: 5' - CAG GGA TCC CTA AAC TCC TCA TCA CCA TCC AC -3'
 3' -GT TAT AGT GCA TGG CCC CGT GAA CTC AGC TGG ACC -5'

Mouse: 5' - CAG GGA TCC AAG CTA CTC ATC ACC ATT CAT G -3'
 3' - G TTA TAG TGG ATG GCC CCC TGA ACT CTT AAG GCC-5'

2.1.1 Polymerase Chain Reaction to Probe cDNA Libraries with $\beta 3$ Integrin Oligonucleotides

Two unique standard PCR solutions were created for the human and mouse samples. Each consisted of 15 μ L 10x PCR buffer, 4.5 μ L dNTPs, 15 μ L FW human (or mouse) diluted stock oligonucleotide, 15 μ L RV human (or mouse) diluted stock oligonucleotide, 7.5 μ L DMSO, 1.5 μ L Pfu Cx Turbo polymerase (Agilent Technologies), and 88.5 μ L ddH₂O. Each standard solution was separated into three PCR tubes, at 49 μ L per tube, plus 1 μ L of the isolated epithelial DNA or cDNA of interest. The final contents of each tube that underwent PCR are shown in Table 2. The samples underwent PCR conditions at 95°C and 72°C, for a total of 30 cycles, and were subjected to a final hold temperature of 4°C. The contents of these tubes were then dyed for visualization and run on a 1.5% (w/v) agarose gel. The results of this gel are shown in Figure 1. These constructs were also verified by sequencing.

Table 2. PCR hybridization tube contents. Each tube contains 49 μ L PCR solution, plus the reagents noted below.

	1	2	3
Human	1 μ L human epithelial cheek cell (personal) DNA	1 μ L 0.328H cDNA	1 μ L human brain cDNA
Mouse	1 μ L mouse brain cDNA	1 μ L 9.5 day mouse cDNA	1 μ L 10.5 day mouse cDNA

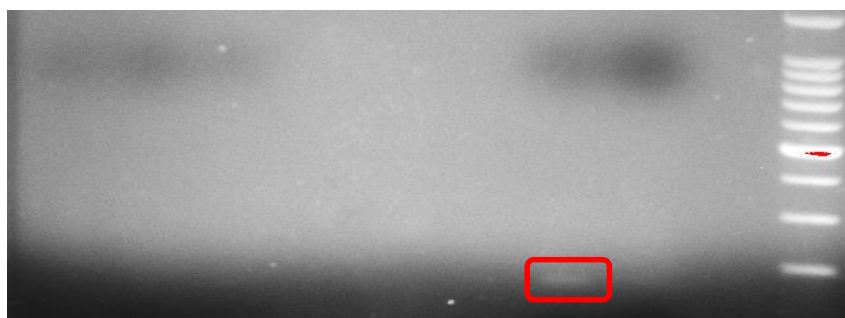


Figure 1. Gel electrophoresis results for presence of β 3 integrin encoding sequence in various human and mouse cDNA samples. The only sample that effectively hybridized to the PCR oligonucleotides was the human brain cDNA (0.328H). The hybridized 0.328H cDNA was then PCR-cleaned using a Promega Wizard® SV Gel and PCR Clean-Up System following the protocol of the manufacturer.

2.2 Expression and Purification of GST β 3 Integrin Fusion Protein

Plasmid vectors pGEX-5X-1 harboring the cytoplasmic region of β 3 integrin were transformed into BL21-Gold (DE3) *E. Coli* cells for the GST protein prep. 12 ml cultures of Luria-Bertani (LB) broth containing ampicillin (Amp) at a concentration of 75 μ g/ml were inoculated with singular colonies of the GST β 3 integrin construct. These cultures were allowed to shake at 220 rpm at 37C for 12-16 hours. 5mL of this culture was then added to a 500 mL LB-ampicillin culture at the same ampicillin concentration, and was allowed to shake at identical conditions. After 90 minutes, and every 20 minutes thereafter, 0.7mL was removed and absorbance was analyzed at A600 nm value using spectrophotometry. Upon reaching an absorbance between 0.5 and 0.8, isopropyl- β -D-thiogalactopyranoside was added to a final concentration of 0.5 mM in the culture. This mixture was then allowed to incubate on the shaker at 220rpm, 37°C for an additional 2.5 to 3 hours. Once evenly divided into three separate bottles, the cultures were centrifuged at 4°C for 15 minutes at 6000rpm. The supernatants were discarded and the bacterial pellets were placed on ice. One pellet was homogenized with 2.5 ml of cold GST Buffer A (2.3 M sucrose, 50 mM Tris pH 7.7, 1 mM EDTA) supplemented with protease inhibitors. 10 ml of cold GST Buffer B (50 mM Tris pH 7.7, 10 mM KCl, 1 mM EDTA) supplemented with 1 mM dithiothreitol (DTT) and protease inhibitors was then added to the second and third pellets to homogenize them as well. 4-5 mg lysozyme (MP Biomedicals) was added to the bacterial culture and allowed to incubate on ice for approximately 1 hour, while swirling every 10 minutes. To this mixture, 175 μ L 10% sodium deoxycholate, 260 μ L 1M MgCl₂, and 25 μ L 5mg/ml DNase I were added and the tube was rocked every two minutes by hand until viscosity significantly decreased. It was then centrifuged at 15,000rpm at 4°C for 40 minutes. Meanwhile, glutathione-sepharose beads were combined with ice-cold 14mL T50ED buffer and were suspended by flicking vigorously, followed by centrifuging at 4°C for 3 minutes at 2200 rpm. This supernatant was discarded, and this wash process was repeated two times. The supernatant of the bacterial tube was then split evenly among the two glutathione-sepharose bead-containing tubes, and they were allowed to rock for 45 minutes in refrigeration. Next, the tubes were spun for 3 minutes at 1300g, 4°C and the supernatant was decanted. 14mL T50ED buffer supplemented with a concentration of 150 mM NaCl was added to each sepharose pellet and flicked to mix. This was centrifuged at 1300g for 3 minutes at 4C, and the supernatant was discarded. After this wash process was repeated three times, the beads were snap frozen in liquid nitrogen, and stored at -80C.

2.4 Co-precipitation Experiments with $\beta 3$ Integrin and G α 12/13

To detect interaction between GST $\beta 3$ integrin lysates and G α 12, G α 13, and their mutants, coprecipitation assays were performed. The G protein lysates were mixed with HEDM buffer and were dispersed evenly into each interaction tube for which it was needed, with the exception of a load tube which contained 30 μ L per protein sample. The GST $\beta 3$ integrin fusion lysates also were suspended in H₅₀E₁D₃M₁₀ (50mM Hepes, 1mM EDTA, 3mM DTT, 10mM MgSO₄) buffer, and 100 μ L was cross applied to each of their interaction tubes (containing G proteins/HEDM), with close attention paid to preventing cross-contamination. These mixtures were allowed to tilt for 90-120 minutes under refrigerated conditions. The tubes were then centrifuged for 3 minutes at 4000rpm, 4°C. The supernatants were mostly discarded, leaving approximately 20 μ L fluid in the tube. 1mL ice-cold HEDLM (HEDM plus added 10% LPX at 1/200th volume) was then added to each sample, and the tubes were inverted ten times. The centrifugation and supernatant partial removal was repeated three times. 1M DTT at a ratio of 1:10 with 4x sample buffer both were mixed in a separate tube. 12 μ L of this mixture was then added to each interaction sample. All tubes were then incubated for 10 minutes at 72°C in a water bath. They were stored at -20°C, until polyacrylamide gel electrophoresis was performed. The resulting immunoblots and Coomassie Blue-stained gels were analyzed for binding affinity and equal distribution of GST-fusion proteins between each interaction tube (see Figure 2). Immunoblot quantitative data was obtained using Kodak GelLogic 100 imaging system and Carestream Molecular Imaging 5.X software to calculate Gaussian fit.



Figure 2. Coomassie Blue stain of GST $\beta 3$ integrin fusion samples confirming integration of the $\beta 3$ integrin coding sequence into the GST-expressing plasmid.

3. Results

To determine whether $\beta 3$ integrin exhibits binding to constitutively active (GTP-bound) G α 12 and G α 13, coprecipitation assays were performed (see Fig. 3). These GTP-bound forms were obtained using a mutational strategy involving a glutamine to leucine (Q229L) switch at amino acid 229 (Q229L). We utilized G α 12- and G α 13-specific primary antibodies to detect binding of the myc-tagged G proteins in our initial experiments, and for our studies directly comparing G α 12 and G α 13 affinity for $\beta 3$ integrin, GFP-tagged variants of these G proteins were utilized and detected them with an anti-GFP antibody. Surprisingly, that G α 13 exhibited impaired binding affinity with both myc- and GFP-tags, while G α 12 exhibited robust binding in both tagged forms.

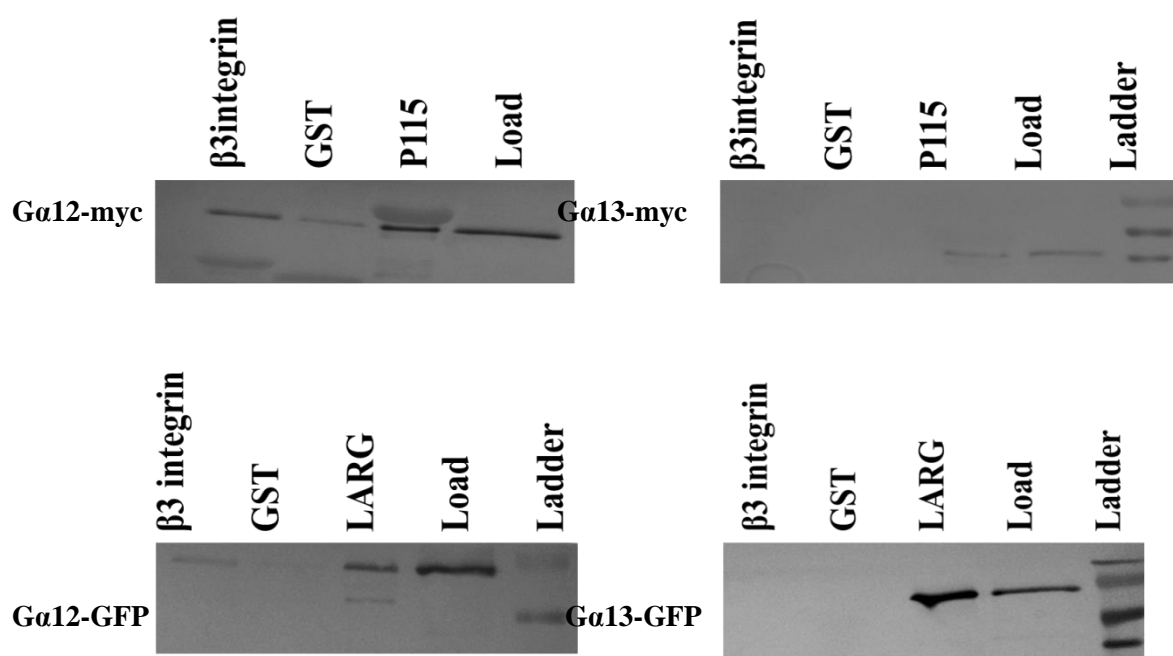


Figure 3. Ga12^{QL} , but not Ga13^{QL} , interacts with $\beta 3$ integrin. The “load” samples serve as a measure of comparative protein abundance, p115 and LARG serve as positive controls, and GST serves as a negative control for $\beta 3$ integrin/ Ga12 pulldown. Immunoblots shown are representative of 3 independent experiments.

To further examine the specific structural determinants within Ga12 that mediate $\beta 3$ integrin binding, NAAIRS cassette substitution mutants were used. To determine the regions within Ga12 specifically responsible for binding affinity of $\beta 3$ integrin, a series of well-tolerated amino acids, asn-ala-ala-ile-arg-ser (NAAIRS), were substituted into various sextuplets of myc-tagged Ga12^{QL} . All mutants were constructed in constitutively active (Q229L) Ga12 . The alphabetical designations of these NAAIRS mutants are depicted in Figure 4, with the Switch I region highlighted in gray¹.

N-terminus — M S G					
V V R T L S	R C L L P A	E A G C A R E	R R A G A A	R D A E R E	A R R R S R
D I D A L L	A R E R R A	V R R L V K	I L L L G A	G E S G K S	T F L K Q M
R I I H G R	E F D Q K A	L L E F R D	T I F D N I	L K G S R V	L V D A R D
K L G I P W	Q H S E N E	K H G M F L	M A F E N K	A G L P V E	P A T F Q L
Y V P A L S	A L W R D S	G I R E A F	S R R S E F	Q L G E S V	K Y F L D N
L D R I G Q	L N Y F P S	K Q D I L L	A R K A T K	G I V E H D	F V I K K I
P F K M V D	V G G Q R S	Q R Q K W F	Q C F D G I	T S I L F M	V S S S E Y
D Q V L M E	D R R T N R	L V E S M N	I F E T I V	N N K L F F	N V S I I L
F L N K M D	L L V E K V	K S V S I K	K H F P D F	K G D P H R	L E D V Q R
Y L V Q C F	D R K R R N	R S K P L F	H H F T T A	I D T E N I	R F V F H A
V K D T I L	Q E N L K D	I M L Q	— C-terminus		

Figure 4. NAAIRS cassette substitution mutants for use in co-precipitation assays.

Since the Switch I region had previously been implicated in binding with cadherins, another class of related cell surface adhesion proteins⁷, NAAIRS mutants spanning this region were tested for similar binding in $\beta 3$ integrin. $G\alpha 12^{QL}$ -myc was used as a positive control, and a blank lysate as a negative control (see Fig. 5). NAAIRS mutant II showed impaired binding to $\beta 3$ integrin as compared with the positive control, and mutant HH showed complete disruption of binding.

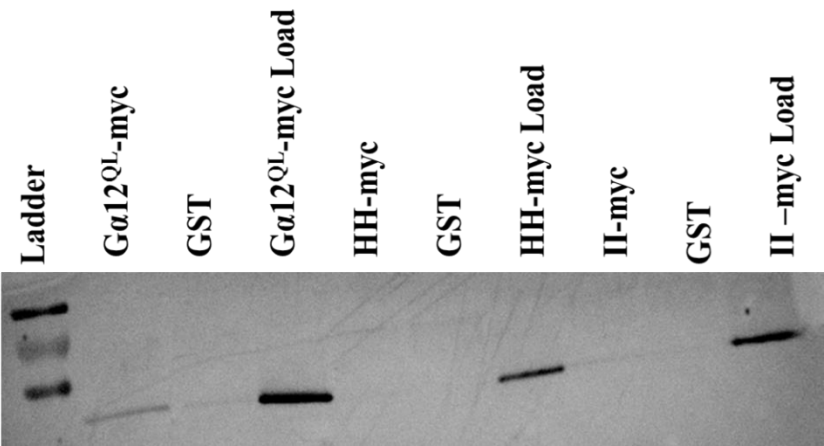


Figure 5. Identification of determinants within $G\alpha 12$ that mediate $\beta 3$ integrin binding. Immunoblots shown are representative of 2 independent experiments.

To determine whether interaction of $\beta 3$ integrin with $G\alpha 12/13$ was reliant on a specific activation state, constitutively active $G\alpha 12^{QL}$ -myc was compared with $G\alpha 12$ wild-type and constitutively inactive (GDP-bound) G228A in co-precipitation experiments. $G\alpha 12^{QL}$ -myc showed greater binding affinity than $G\alpha 12$ wild-type or G228A. $G\alpha 13$ did not display any detectable binding, regardless of activation state (see Fig. 6a). Quantification of binding data was also performed for these two co-precipitation assays. Gaussian fit values were determined for bands on immunoblots and used to calculate precipitate-to-load densitometric ratios (Fig. 6b).

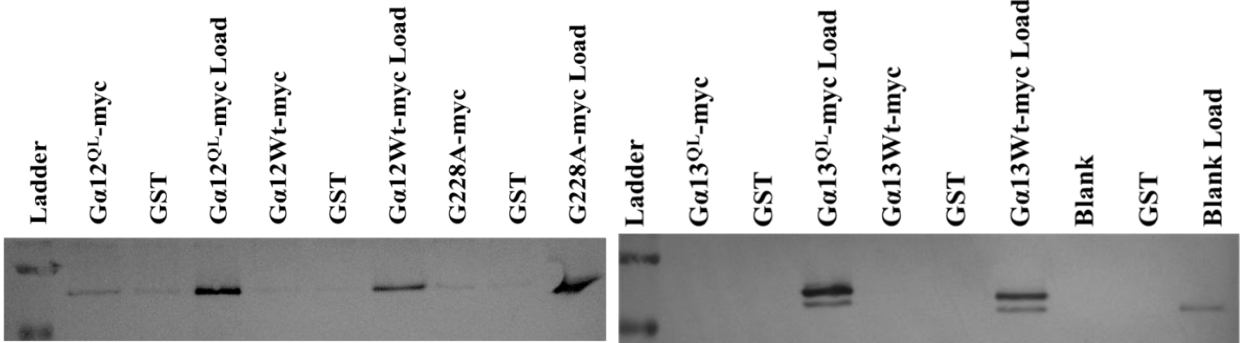


Figure 6a. Activation dependence for $\beta 3$ Integrin interaction. Immunoblots shown are representative of 3 independent experiments.

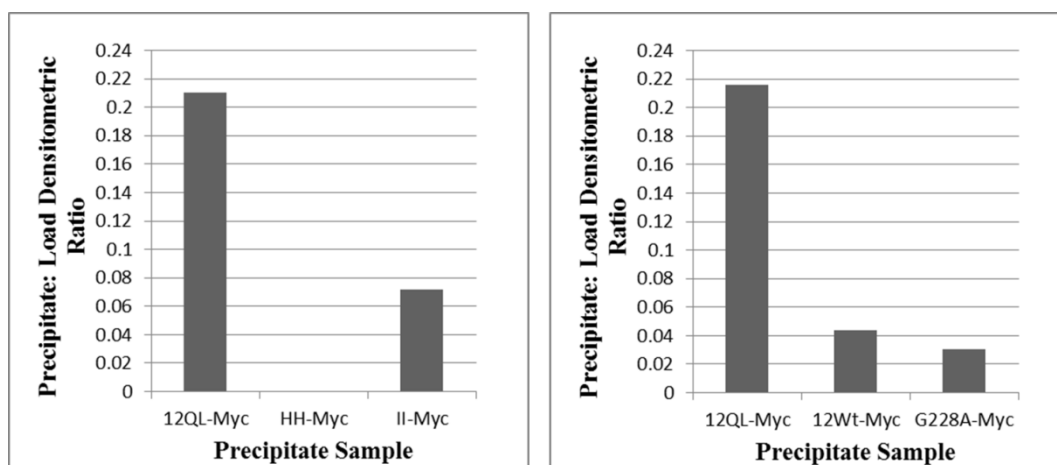


Figure 6b. Precipitate-to-Load Densitometric Data

4. Discussion

Unexpectedly, myc-tagged $\alpha 12$, but not myc-tagged $\alpha 13$, interacted with $\beta 3$ integrin. This was similarly demonstrated in that $\alpha 12$ -GFP interacted with $\beta 3$ integrin whereas $\alpha 13$ -GFP did not. Therefore, $\alpha 13$ exhibits impaired binding affinity with both myc- and GFP-tags, suggesting that it is not a function of epitope tag blocking binding but rather that the protein as a whole does not interact with $\beta 3$ integrin in the constitutively active state. This implicates data never before elucidated about the binding capabilities of $\beta 3$ integrin, and suggests that $\alpha 12$ plays a greater role in $\beta 3$ integrin interaction than does $\alpha 13$. This could be especially significant not only due to the potential for the crosstalk of downstream pathways, but for the direct physical binding effects that may arise from this interaction. As has been previously shown, when $\alpha 13$ is bound to $\beta 3$ integrin, c-Src is active, RhoA is inhibited, and platelet spreading occurs⁴. This implies that the basic, physical interaction of the G protein with $\beta 3$ integrin bolsters the natural activity of integrins, which may be clinically applicable in a medical setting. Further elucidation of how this physical binding affects either $\beta 3$ integrin or $\alpha 12$ is needed, and could be completed by testing known binding targets of $\beta 3$ integrin such as Talin, to see if activity is inhibited or stimulated⁸.

Co-precipitation assays with Switch I region NAAIRS mutants displayed similarly interesting data regarding the uniqueness of $\beta 3$ integrin interaction with G proteins. The impairment seen in NAAIRS region II and complete blockage in region HH is interesting in comparison to binding exhibited by cadherins. Previous data suggests these regions (within Switch I) of $\alpha 13$ are potentially necessary for binding to vascular endothelial (VE) cadherin⁷. Thus, we may conclude that the Switch I regions in both $\alpha 12$ and $\alpha 13$ evolutionarily represent integral and relatively functionally unchanged domains, as they both seem to be necessary for the binding of these cell surface adhesion proteins.

Upon performing activation state co-precipitation assays, it became apparent that activation state had little effect on the binding capabilities of $\beta 3$ integrin and $\alpha 12/13$ proteins. This serves as further evidence that the results achieved describing the impaired binding of $\alpha 13$ with $\beta 3$ integrin is generalized. The disparity in the data between our lab and that of previous researchers may have to do with the activation mutagenesis strategy used. In the Meigs lab, a Q229L point mutation strategy in $\alpha 12/13$ was employed, whereas others have used a truncation strategy to test interaction⁴.

Further directions for this research include a further comparative pulldown of $\alpha 13$ including G225A (constitutively inactive), to determine if an inactive (GDP-bound) form is capable of interaction with $\beta 3$ integrin. To better elucidate which structural determinants of $\alpha 12$ confer binding specificity with $\beta 3$ integrin, further studies with NAAIRS mutant co-precipitation including within and flanking the Switch I Region may be completed. Additionally, the use of $\alpha 12/\alpha 13$ chimeras may reveal the structural basis of preferential $\alpha 12$ binding to adhesion proteins. Lastly, studies of the cell biological role of $\alpha 12$ - $\beta 3$ integrin interaction using selectively uncoupled $\alpha 12$ mutants and inhibitory peptides may also confer novel data about $\beta 3$ integrin and what physiological implications it may have.

6. Acknowledgements

The author would like to acknowledge the invaluable support and guidance of Dr. Thomas E. Meigs in his procedural insight and analysis of experimentation, as well as the financial support by GlaxoSmithKline, Faculty Research Grants, and the UNC Asheville Undergraduate Research Program. Further thanks goes to Jonathan Sims in his tandem research with cadherins and assistance with organization and presentation of this project, as well as past lab member Kayla Huffman for related research.

7. Resources

1. Ritchie, B.J., Smolski, W.C., Montgomery, E.R., Fisher, E.S., Choi, T.Y., Olson, C.M., Foster, L.A., Meigs, T.E. (2013). Determinants at the N- and C-termini of Ga12 required for activation of Rho-mediated signaling. *Journal of Molecular Signaling*, 8.
2. Meigs, T.E. and A. Lyakhovich. (2012). G Protein Alpha 12. *Encyclopedia of Signaling Molecules*.
3. Shen, B., Delaney, M.K., and X. Du. (2012). Inside-out, outside-in, and inside-outside-in: G protein signaling in integrin-mediated cell adhesion, spreading, and retraction. *Current Opinion in Cell Biology*, 24, 600-606.
4. Gong, H., Shen, B., Flevaris, P., Chow, C., Lam, S., Voyno-Yasnetskaya, T.A., Kozasa, T., and Du, X. (2010). G Protein Subunit Ga13 Binds to Integrin α IIb β 3 and Mediates Integrin "Outside-In" Signaling. *Science*, 327, 340-343.
5. Shen, B., Zhao, X., O'Brien, K.A., Stojanovic-Terpo, A., Delaney, M.K., Kim, K., Cho, J., Lam, S., and X. Du. (2013). A directional switch of integrin signaling and a new anti-thrombotic strategy. *Nature*, 503, 131-136.
6. Vinogradova, O., Velyvis, A., Velyviene, A., Hu, B., Haas, T., Plow, E., and Qin, J. (2002). A structural mechanism of integrin α (IIb) β (3) "inside-out" activation as regulated by its cytoplasmic face. *Cell*, 10(5), 587-97.
7. Gong, H., Gao, X., Feng, S., Siddiqui, M., Garcia, A., Bonini, M.G., Komarova, Y., Vogel, S.M., Mehta, D., Malik, A.B. (2012). Evidence of a common mechanism of disassembly of adherens junctions through Ga13 targeting of VE-cadherin. *Journal of Experimental Medicine*, 211(3), 579-581.
8. Shattil, S.J., Kim, C., Ginsberg, M.H. (2010). The final steps of integrin activation: the end game. *Nature Reviews Molecular Cell Biology* 11, 288-300.